# EXPERIMENTAL STUDY ON PLASTIC DEFORMABILITY OF HIGH STRENGTH PRESTRESSED CONCRETE PILES UNDER AXIAL AND LATERAL FORCES

by Seiji Kokusho (I), Akira Wada (I), Katsumi Kobayashi (I)
Shizuo Hayashi (II), Masahiro Horii (III), Hiromi Kihara (III)
Seiji Saito (IV)
Presenting Author: Hiromi Kihara

## SUMMARY

Reported in this presentation are the results of bending shear tests carried out for various test specimens of high-strength prestressed concrete piles of which amount of longitudinal PC bars, extent of pre-stressing of concrete, and amount of spiral anti-shear reinforcement are varied, and on the test specimens of which PC bars are replaced with deformed bars. These tests were carried out to confirm plastic deformability of high-strength prestressed concrete piles.

## INTRODUCTION

### History of Making High-Strength Prestressed Concrete Pile for Practical Use

The majority of Japanese cities are located on alluvial plains facing the coast. Therefore, it is the general practice to adopt pile foundations for constructing heavy buildings on such alluvial plains because of the existing weak stratum. Piles used for the purpose nowadays are classified into: (1) molded reinforced concrete piles at the construction site by pouring concrete, and (2) pre-cast concrete piles, such as high-strength prestressed concrete piles.

Reviewing the development of pre-cast concrete piles in Japan, castings of centrifugal reinforced concrete piles were first made in 1933, and then the casting of high-strength prestressed concrete piles were made. It is said that prestressed concrete piles were first used for bridge piers constructed in seawater for building expressways in 1962. High-strength prestressed concrete piles were made practical in 1967, and three types of high-strength prestressed concrete piles, namely 40, 80 and 100 $kg/cm^2$ according to the extents of prestressing, have been specified by the Japanese Industrial Standards (JIS) since 1982. High-strength PC piles are widely used in Japan.

### Aseismic Designing of Superstructures and Countermeasures against Earthquakes

Since Japan is one of the most earthquake-prove countries in the world, aseismic laws and regulations are laid down. Allowable Unit Stress Designing Method (Law to design the structure to be elastically durable against lateral force corresponding to 20% of the weight of the bulding), which was laid down based on the knowledge gained from the Great Kanto Earthquake (1923), has been enforced for 50 odd years. However, recon-sideration of the current laws and regulations was commenced after the bitter experience of the severe damage to building from the Offshore Tokachi Earthquake in 1968 and new laws and regulations have been laid down since 1981 taking various results of researches and new knowledge [Ref. (1)].

(I) Tokyo Institute of Technology, Tokyo, Japan
(II) Fukui University, Fukui, Japan
(III) Nikken Sekkei Ltd., Tokyo, Japan
(IV) Maeta Concrete Works Ltd., Tokyo, Japan

Distinctive features of the new aseismic laws and regulations on superstructures (building) are roughly summarized into two as follows.

a. Earthquake motions are classified into two stages as follows:

   i) There should be no damage to any buildings by medium or small earthquakes (Surface Acceleration: 80 - 100 gal).
   ii) There should be no collapse of buildings or human insury even in a large earthquake (300 - 400 gal).

b. In order to make the performance of the structure satisfy the requirements in a. above, allowable unit stress designing is made on the structure so that it can endure a seismic force of 0.2G of Baseshear Coefficient which corresponds to medium/small earthquakes. Although seismic force of 1.0G of Baseshear Coefficient is assumed to correspond to a large earthquake, aseismic durability of each structural member and framework is confirmed so that retained horizontal strength of the framework is maintained within the range of 0.25 - 0.55G by applying retained horizontal strength reduction coefficient corresponding to their plastic deformabilities, according to such analysis methods as Yield Hinge Method, etc.

On the other hand, institutionalization of aseismic laws and regulations for foundational structures has been delayed because of the complexity of earthquake phenomena. At present, it is limited just to confirming that the stress applied to the pile by the horizontal force corresponding to the base shear of the building (0.2 G.W.) by medium or small earthquakes is lower than the allowable stress. However, destructive earthquakes occurred very often in Japan. Although no remarkable damages were observed by those earthquakes to the structures, several examples of brittleness destruction of piles were reported because their ultimate stresses were exceeded by the stresses applied to them [ Ref. (2)].

For improving aseismic performances of foundational structures, especially those of piles, possible measures to be taken are to increase the number of piles, or to use piles of higher strength. However, such measures increase the construction cost. Therefore, one of the effective measures to be taken for improving aseismic performance of piles would be to use that of large plastic deformability after the stresses applied to piles by the seismic force reached their ultimate stresses. Refer to Reference (3) for the details of the aseismic designing of PC piles applied in the U.S.

### Purpose of the Experimental Work

The purpose of this experimental work is to find a clue for manufacturing piles of higher resilience, by grasping plastic deformabilities of current high strength prestressed concrete piles through the experimental work.

## OUTLINE OF THE EXPERIMENTAL PLAN

### Test Specimens

All of the test specimens used for this experimental work were high strength concrete piles with outer diameter of 30 cm, and hollow cylindrical structure with wall thickness of 6 cm. They are classified into three as follows:

PC bars were used for P Series specimens and PN Series specimens as longitudinal reinforcements. PC bars were replaced with deformed bars in R Series specimens.

Difference between P Series specimens and PN Series specimens is the presence or absence of axial force as external force in them.

Details of those series of specimens are as follows:

a. P Series Specimens: The number of PC bars for longitudinal reinforcements was decided according to A, B, and C grades of JIS Specifications. Effective prestresses applied to specimens were 100, 80 and 40 kg/cm$^2$, which were the upper limits stipulated in JIS Specifications and 0 kg/cm$^2$. Although the standard spiral hoop of 3.2 mm$\phi$ @100 mm was used for high strength PC piles, spiral hoop of 4.0 mm$\phi$@50 mm which was about three times amount of standard spiral hoop was used in PC' Series specimens (Table 1).

b. R Series Specimens: Longitudinal reinforcements were made by other materials of which the product of gross area and yield strengths ($Ag \cdot s\sigma y$) are similar to that of PC bars. No prestressing was applied to the specimens (Table 2).

c. PN Series Specimens: Same as P Series specimens except for their lengths. However, axial loads were applied to these specimens by placing PC bars of larger diameter (40 mm$\phi$) in their hollow portion. The axial forces of the specimens were 35 tonf and 70 tonf which corresponded to the allowable tip bearing power of piles respectively, in the soil bearing layer of which N value by the Standard Penetration Test (SPT) was 50 (Table 3).

<u>Testing System</u>

Experimental device is shown in Fig. 1 and Photo. The loading system was of simple beam concentrated load assuming the stress to be caused nearby the head of high strength PC piles which were fixed to the foundation. Shear span ratio (M/QD) of 3 was adopted for the test, because shear span ratios of normal pile foundation were obtained within the range of 2 - 3.5 when their heads were fixed. Lengths of specimens were decided so that their bending moment at their center by their empty weight became zero. Applied load (horizontal force) was toward one direction.

Load was applied to the steel band (width: 12 cm, thickness: 4.5 mm) processed so as to match the outer diameter of the pile, lest loading tool should damage the pile specimen and taking possible application of horizontal force at the connecting point of pile and foundation into consideration. Supporting point made of concave steel lined with buffer rubber sheet was used, and the pin-roller conditions were satisfied by setting a semicircular pin and slide needle bearing there.

<u>Measurement Method</u>

Measurements of deflection of pile specimens were made by electric transducer fixed with gauge holder supported at the upper part of the supporting points of the test specimen. Strain was measured by strain gauge which was stuck on the concrete surface.

## TEST RESULTS

<u>P Series Specimens</u>

Shown in Fig. 2 - Fig. 5 are the relations between applied load P and extent of deformation at the loading point.

(Bending Loads that cause Cracking)
Bending loads that cause cracking indicate linear relation with the extents of effective prestress in all of the test specimens. Remarkable deformation was observed on PA Series test specimens after the generation of cracks because of lesser amount of longitudinal reinforcement.

(Maximum Load)
It is understood that the maximum load is proportional to the extent of amount of longitudinal reinforcement and does not depend on effective prestress. However, any test specimen which incurred shear destruction before the bending destruction cannot indicate the same ultimate strength as other specimens containing the same amount of longitudinal reinforcement.

(Plastic Deformability)
This is a common phenomenon observed in all of the test specimens.
However, more deformation is observed under the maximum load on the test specimen of which effective prestressing has been decreased to improve its plastic deformability. Test specimens which contain less spiral anti-shear reinforcement tend to incur shear destruction before the damage of longitudinal reinforcement. Thus, their deformability cannot be improved even though they are prestressed to a lesser extent.

(Destructive Mode)
Destructive modes of test specimen can roughly be classified into two, namely destruction of longitudinal PC bar and destruction of spiral anti-shear reinforcement.
Specimens marked with B in the Fig. 2 $\sim$ 10 (PA-0, 40; PB-40, 80; PC'-0, 80, 100) lost their strength because widths of cracks just under the loading point are increased and axial loads are fractured. However, no collapse is observed on the concrete of compressed side of PA Series test specimens, which contained less longitudinal reinforcements, and axial loads of all of the other test specimens were destroyed after they collapsed.
Spiral hoops of test specimens marked with S (PB-0, PC-Series, PC'-40) were fractured after the width of their diagonal cracks increased. However, no collapse of concrete was observed on test specimen PB-0 which contained less longitudinal reinforcement.

(Generation of Cracks)
Observing the generation of cracks on the test specimens, it can be said that extremely few cracks are observed on AP Series test specimens, which contain less axial loads, than those of PB, PC, and PC' Series.

R Series

Shown in Fig. 6 - Fig. 8 are the relations between applied load P and extent of deformation at the loading point. The dotted line in the figures is the relation between P and $\delta$ of P Series specimens in which effective prestress are maximum (PA-40, PB-80, PC-100).

(Bending Loads that cause Cracking)
Bending loads that cause cracking in all of six test secimens were found to be almost equal which nearly coincided ith the results obtained on the P Series specimens in which prestress was not introduced.

(Maximum Load)
Maximum load depended on the extent of longitudinal reinforcement and was not overly affected by the extent of spiral reinforcement. A possible reason why the

maximum load was obtained larger than that of high strength PC pile of which yield strength ($Ag \cdot s\sigma y$) of longitudinal reinforcement was almost identical could be the smaller yield ratio of deformed bar. That is to say, such a phenomenon could be due to larger destruction strength of test specimen compared to its yield point, as shown in Table 4.

(Plastic Deformability)
It was clarified that considerably better deformabilities were obtained on the test specimens containing longitudinal reinforcement with deformed bars except specimen RC-0 than those of P Series test specimens. This is possibly because the unit strength of the specimen continued to increase even after the yield of the reinforcement at the section of the loading point due to smaller yield ratio of deformed bar, and the yield of the reinforcement proceeded from the central portion toward both ends to generate cracks covering a wide area. The test specimen RC-0, which contained less spiral reinforcement compared to its bending strength, was shear destructed under smaller deformability than other test specimens.

PN Series

These are the test specimens loaded an axial force by placing PC bar of 40 mmø in their hollow portion. Shown in Figs. 9 and 10 are the relations between load $P_1$ and the extent of deformation $\delta$ at the loading point. Since the axial force by PC bars in PN Series test specimens are made eccentric by their deformation, the applied load P was corrected to be expressed by $P_1$ after converting the extent of eccentricities into bending moments.

(Maximum Load and Failure Mode)
Test specimens with axial force of 35 tonf as external force indicate nearly constant maximum load regardless of the extent of prestress applied to them. Although test specimens with axial force of 70 tonf also indicate nearly constant maximum load, the value of maximum load is larger than that of the test specimen with axial force of 35 tonf.
Test specimens with axial force of 35 tonf caused fracture of longitudinal tension bars due to bending moment. However, only test specimen PNB-40-35, which contained less spiral hoop and was prestressed to a lesser extent, caused shear fracture because the spiral hoop was fractured after the bending yield. All of test specimens with axial force of 70 tonf caused compression failure of concrete due to bending moment rapidly.

(Plastic Deformability)
Although test specimens with axial force of 35 tonf and those with 70 tonf are destroyed in different mode, there is no remarkable difference in the deformation under maximum load and in the plastic deformability between the two. Their deformabilities are largely deteriorated compared to those of P Series test specimens without axial force. A possible reason why poor deformability of test specimen with axial force of 35 tonf is observed despite the fact that its failure mode is of rupture of bending tensile reinforcement could be the smaller difference between the maximum load and the cracking load by bending and due to narrow crack generation zone (the zone in which the longitudinal reinforcement has been yielded).

## CONCLUSIONS

a. Although the cracking load by bending directly depends on the amount of prestress, ultimate bending strength is proportional to the extent of longitudinal reinforcement and does not directly depend on the amount of prestress. Taking this into consideration, prestress can be introduced in the pile construction to the extent that it vents the generation of cracks against the bending moment caused by medium or small earthquakes, and the ultimate strength of the pile can be enlarged by arrangement of a necessary extent axial loads instead of expecting an effect of great amount of prestress against large earthquake motions.

b. If the shear span ratio is kept at 3.0 as in this experiment, current high strength prestressed concrete piles incorporating spiral hoop to satisfy the minimum requirement of JIS Specification, which is 3.2 mmϕ @100 mm ($P_W = 3.14 \times 0.32^2/4 \times 6 \times 10 = 0.13\%$), may cause shear failure due to rupture of the spiral hoops. It was revealed that increasing the extent of spiral hoop was effective for preventing shear failure of PC piles, by comparing test results of PC Series test specimens with those of PC' Series, and by comparing those of PNB Series and PNB' Series.

c. High strength prestressed concrete piles cause shear failure at an earlier stage if their concrete stresses are kept zero. At the same time, those with excessively large longitudinal reinforcements would be fractured rapidly due to compression failure of concrete. Therefore, it is necessary to give careful considerations in designing buildings if considerable variations of axial forces of piles are anticipated during earthquakes.

d. According to the test results obtained on test specimen PNB-80-35, it can be said that the ultimate strength of B grade high strength prestressed concrete piles which satisfy the current JIS Specifications is obtained at around 0.41G (29 tonf/2 x 35 = 0.41) converting into horizontal force. However, once any building with larger horizontally resisting strength of superstructure is exposed to a large earthquake, the building may not be able to withstand the earthquake only with strength of piles and, furthermore, it cannot be said that the deformability of such piles is sufficient.

Acknowledgements

The authors would like to thank Prof. H. Kishida, Tokyo Institute of Technology, Mr. H. Fujii and Mr. S. Kon, Maeta Concrete Works Ltd. and Mr. H. Take, Shimizu Construction Co., Ltd.for their kind suggestions.

References

(1) "A Proposal of a New Aseismic Design Method for Building in Japan", by Kiyoshi Nakano at Proceedings of the Seventh WCEE, Vol. 4.

(2) "Damage of Reinforced Precast Piles during the Miyagiken-Oki Earthquake of June 12, 1972" by Hideaki Kishida et al - Proceedings of the Seventh WCEE, Vol. 9.

(3) "Seismic Design of Prestressed Concrete Piling" by David Sheppard, PCI Journal, Vol. 28, No. 2, March/April, 1983.

Table 1 List of P-series speimens

| specimens | effective prestress (kg/cm²) | longi. bars | spiral bars |
|---|---|---|---|
| PA -0<br>PA -40 | 0<br>40 | 6-7.4φ | 3.2φ-@100 |
| PB--0<br>PB -40<br>PB -80 | 0<br>40<br>80 | 8-9.2φ | 3.2φ-@100 |
| PC -0<br>PC -40<br>PC -80<br>PC -100 | 0<br>40<br>80<br>100 | 10-9.2φ | 3.2φ-@100 |
| PC'-0<br>PC'-40<br>PC'-80<br>PC'-100 | 0<br>40<br>80<br>100 | 10-9.2φ | 4.0φ-@ 50 |

Photo of testing system

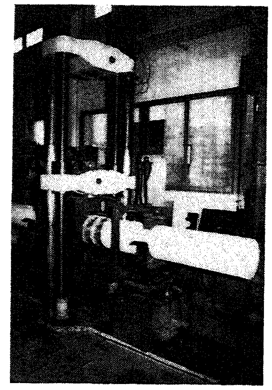

Table 2 List of R-series specimens

| specimens | effective prestress (kg/cm²) | longi. bars | spiral bars |
|---|---|---|---|
| RA -0<br>RA'-0 | 0 | 10-D13 | 3.2φ-@100<br>4.0φ-@ 50 |
| RB -0<br>RB'-0 | 0 | 16-D13 | 3.2φ-@100<br>4.0φ-@ 50 |
| RC -0<br>RC'-0 | 0 | 14-D16 | 3.2φ-@100<br>4.0φ-@ 50 |

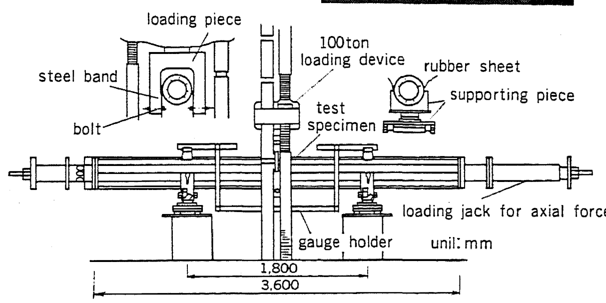


Fig. 1 Testing system

△ bending crack
▲ compression failure
Ⓑ— rupture of longitudinal bars
Ⓒ— failure of concrete at compression side
Ⓢ— rupture of spiral bars

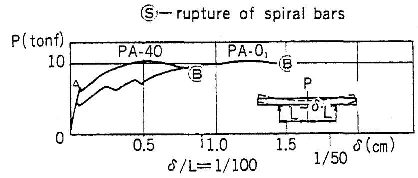


Fig. 2 P-δ relations of PA series

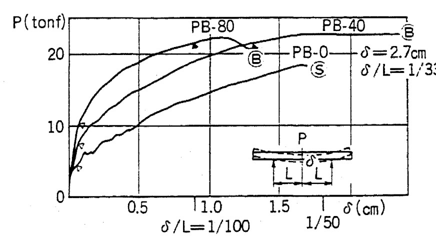


Fig. 3 P-δ relations of PB series

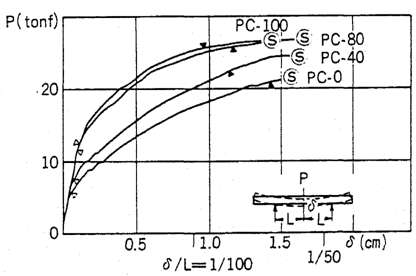


Fig. 4 P-δ relations of PC series

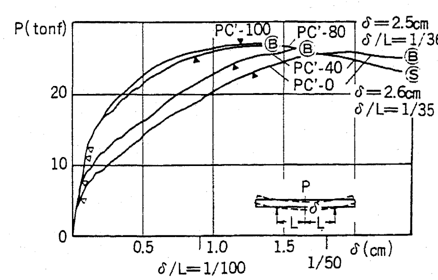


Fig. 5 P-δ relations of PC' series

Table 3 List of PN-series specimens

| specimens | effective prestress (kg/cm²) | longi. bars | spiral bars | Axial Force (tf) |
|---|---|---|---|---|
| PN -40 | 40 | 9-7.2φ | 3.2φ-@ 100 | 35 |
| PN -80 | 80 | 8-9.2φ | 3.2φ-@ 100 | |
| PN'-40 | 40 | 8-9.2φ | 4.0φ-@ 50 | |
| PN'-80 | 80 | 8-9.2φ | 4.0φ-@ 50 | |
| PN -40 | 40 | 8-9.2φ | 3.2φ-@ 100 | 70 |
| PN -80 | 80 | 8-9.2φ | 3.2φ-@ 100 | |
| PN'-40 | 40 | 8-9.2φ | 4.0φ-@ 50 | |
| PN'-80 | 80 | 8-9.2φ | 4.0φ-@ 50 | |

Table 4 Properties of Longitudinal Reinforcement

| specimens (longi. bars) | | ag (cm²) | sσy (tf/cm²) | ag*sσy (tf) | sσb (tf/cm²) | ag*sσb (tf) | elongation (%) |
|---|---|---|---|---|---|---|---|
| PA -series | (7.4φ) | 3.4 | 14.8 | 35.5 | 15.1 | 36.2 | 9.5 |
| PB -series<br>PN -series<br>PN'-series | (9.2φ) | 5.1 | 14.0 | 71.4 | 15.0 | 76.5 | 8.0 |
| PC -series<br>PC'-series | | 6.4 | | 89.6 | | 96.0 | |
| RA -series<br>RA'-series | (D-13) | 12.7 | 3.74 | 47.5 | 5.56 | 70.6 | 25.6 |
| RB -series<br>RB'-series | | 20.3 | | 75.9 | | 112.9 | |
| RC -series<br>RC'-series | (D-16) | 27.8 | 3.79 | 105.4 | 5.76 | 160.1 | 24.1 |

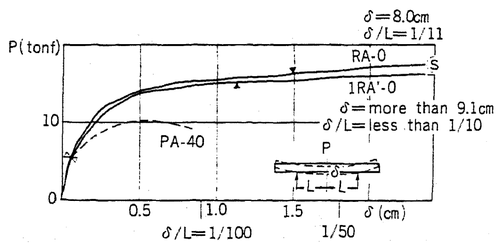


Fig. 6 P-δ relations of RA, RA' series

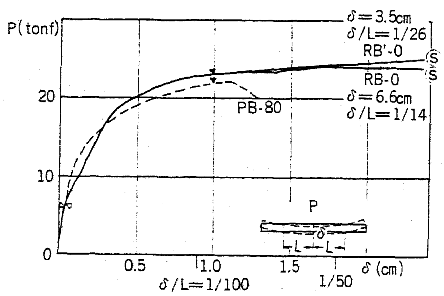


Fig. 7 P-δ relations of RB' series

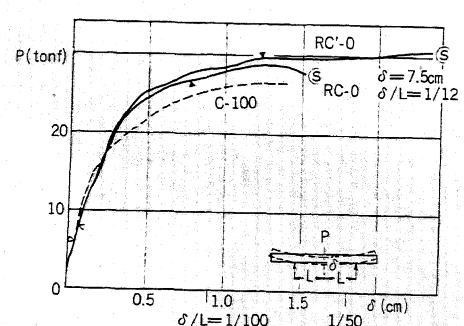


Fig. 8 P-δ relations of RC, RC' series

△ bending crack
▲ compression failure

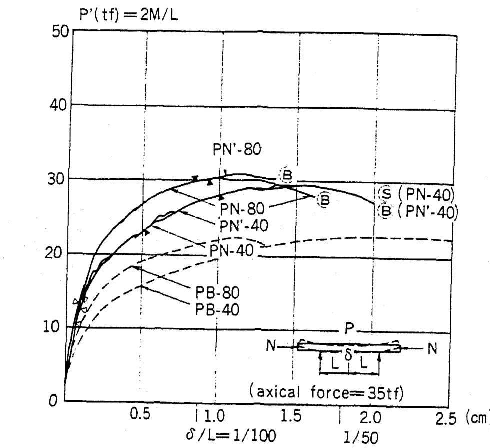


Fig. 9 P-δ relations of PN series (N = 35tf)

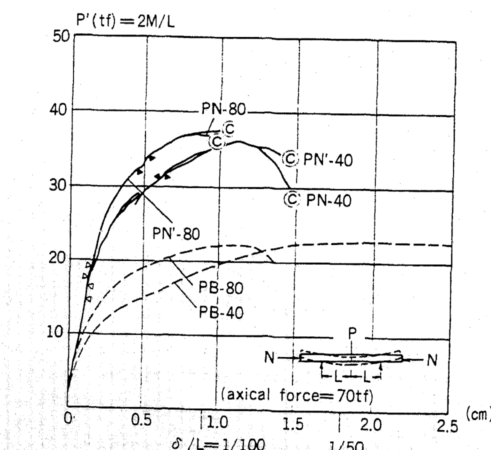


Fig. 10 P-δ relations of PN series (N = 70tf)

△ bending crack
▲ compression failure